Vision-Based Horizon Extraction for Micro Air Vehicle Flight Control

Gui-Qiu Bao, Shen-Shu Xiong, *Member, IEEE*, and Zhao-Ying Zhou

***Abstract*—Recently, more and more research has been done on micro air vehicles (MAVs). An autonomous flight control system is necessary for developing practical MAVs to be used for a wide array of missions. Due to the limitations of size, weight, and power, MAVs have the very low payload capacity and moments of inertia. The current technologies with rate and acceleration sensors applied on larger aircrafts are impractical to MAVs, and they are difficult to be scaled down to satisfy the demands of MAVs. Since surveillance has been considered as the primary mission of MAVs, it is essential for MAVs to be equipped with on-board imaging sensors such as cameras, which have rich information content. So vision-based techniques, without increasing the MAVs payload, may be a feasible idea for flight autonomy of MAVs. In this paper, a new robust horizon extraction algorithm based on the orientation projection method is proposed, which is the foundation of a vision-based flight control system. The horizon extraction algorithm is effective for both color images and gray images. The horizon can be extracted not only from fine images captured in fair conditions but also from blurred images captured in cloudy, even foggy days. In order to raise the computational speed to meet real-time requirements, the algorithmic optimization is also discussed in the paper, which is timesaving by narrowing the seeking scope of orientations and adopting the table look-up method. According to the orientation and position of the horizon in the image, two important angular attitude parameters for stability and control, the roll angle and the pitch angle, could be calculated. Several experimental results demonstrate the feasibility and robustness of the algorithm.**

***Index Terms*—Control, horizon extraction, micro air vehicles (MAVs), vision.**

I. Introduction

SINCE the 1990s, many researchers have been interested in micro air vehicles (MAVs), a class of small low-flying aircrafts that are significantly smaller than currently available remotely piloted vehicles. Equipped with small video cameras and transmitters, MAVs will complete a number of important missions for monitoring tasks, such as remote sensing, surveys of disaster areas, accident reconnaissance, forest-fire surveillance, etc. [1]–[4]. In order to be used for a wide array of missions, MAVs should be equipped with autonomous capabilities. An autonomous flight control system is necessary for developing practical MAVs, while the angular orientation measurement is the basis for achieving MAV autonomy. For larger aircrafts, the angular attitudes are typically estimated by the integration of the aircraft's angular rates or accelerations from inertial sensors. Classically, high-precision gyros are required, which are large and heavy. The attitude problem has also been solved by an attitude heading reference system (AHRS) using gyros that are updated by gravity sensors (pitch and roll) and magnetic field sensors (yaw) with low-pass filters to attenuate errors incurred during turns. Successful AHRSs require very expensive sensors with high performance that have exceptional long-term bias stability and inevitably suffer from large size and heavy weight. The mass and cost of sensors restrict these technologies to applications in MAVs. Thus, the current technologies with rate and acceleration sensors on larger aircrafts are impractical to MAVs.

Although MEMS rate gyros, accelerometers and magnetometers are small enough to be carried by MAVs, their accuracy is not high for reduced size and weight. MEMS rate gyros are highly sensitive to the temperature change and exhibit poor long-term bias stability. Due to small scales, MAVs have low moments of inertia, which make them sensitive to rapid angular accelerations. The attitudes of MAVs usually change frequently and even dramatically. It is hard to measure the gravity acceleration vector accurately in high dynamic maneuvers. So the current technologies used on larger aircrafts are difficult to be scaled down to satisfy the demands of MAVs. The attitude determination for MAVs remains an open topic. However, MAVs angular orientation information is required by the stability and control of MAVs, which is the basis of autonomous flight. Thus, autonomous flight control of MAVs presents some difficult challenges.

Since surveillance has been considered as the primary mission of MAVs, it is essential for MAVs to be equipped with on-board imaging sensors such as cameras, which have rich information content. Vision-based techniques using present imaging sensors without extra increasing the MAVs payload may be a feasible idea for flight autonomy of MAVs. Some computer vision technologies have been adopted in control and navigation of air vehicles. Several vision systems have been reported for providing autonomous aircrafts with visual perception for such tasks as object recognition and attitude determination, six degrees of freedom (6DOF) estimation with respect to landmarks and navigation parameter identification from sequential aerial images. In [5], the status of an ongoing project is described whose goal is to develop a prototype vision system that can support at least navigation and possibly object recognition and pose estimation in MAVs. The work consisted of two parts: range-based vision for object recognition and pose estimation, and monocular vision for navigation and collision avoidance. The monocular navigation system is based on finding corresponding features in successive images and deducing from these the partial or complete relative pose of the aircraft. The methods are under development based on

Manuscript received June 15, 2003; revised December 10, 2004.

The authors are with the Department of Precision Instruments, Tsinghua University, Beijing 100084, P.R. China (e-mail: xiongss@mail.tsinghua.edu.cn).

Digital Object Identifier 10.1109/TIM.2005.847234

detecting and registering horizon pixels in two consecutive images. Three angular pose parameters could be estimated based on horizon registration. To label a given pixel as a horizon pixel, the condition that in the blurred image the gray-level gradient in the vertical direction should be sufficient large is required to be satisfied. The horizon pixels are extracted by traveling down along every column. In [6], the authors present an optical landing system that obtains orientation information for an aircraft based on visual data and stored information about the particular landmark "runway." The orientation information for the aircraft, including 6DOF of the aircraft that are x, y, z positional information and roll, pitch and yaw attitude information, is determined by using a stored description of the runway dimensions and the runway features extracted from the video image produced from a forward-looking camera. In [7], a vision-based horizon-tracking control system is developed for MAVs, which is based on a statistical horizon detection algorithm. The algorithm attempts to minimize the intra-class variance of the ground and sky pixel distributions. One of the basic assumptions is that the horizon will separate the image into two regions which have different appearance. For the purpose, the color defined in RGB space is viewed as the most important measurement of appearance. For any given hypothesized horizon line, the pixels above the line and below the line are labeled as the sky and the ground, respectively. The optimization criterion is defined according to the covariance matrices of the two pixel distributions. The horizon is the line that maximizes the optimization criterion. A simple PD controller is employed to validate vision-based flight stability and control for MAVs. In [8], a hybrid method for navigation parameter estimation using sequential aerial images is proposed. The navigation parameters represent the position and velocity information of an aircraft for autonomous navigation. The proposed system is composed of two parts: relative position estimation and absolute position estimation. Reference images or digital elevation model information is needed in the algorithm. The vision-based navigation system suggested in [9] determines the 18 states by combining conventional aircraft sensors like gyros, accelerometers, artificial horizon, aerodynamic measuring devices and GPS with vision data taken by conventional CCD-cameras mounted on a pan and tilt platform.

In our research work about vision-based flight control, the basic information to be extracted from the visual signal of an on-board camera is the MAVs orientation information including angular attitude parameters and altitude information, while the angular orientation determination is the foundation of a flight stability and control system. The horizon could provide the farthest and the most stable objects in the image captured from a forward facing camera on the MAV [5]. And two important angular attitude parameters for stability and control, the roll angle and the pitch angle, could be derived from the slope and the position of a line corresponding to the horizon in the image. Thus detecting horizon lines in video images as seen from a forward-looking camera is the basis of our developed vision-based attitude determination system. In this paper, a new robust horizon extraction algorithm based on the orientation projection method is suggested, which makes full use of orientation information of the images. The algorithm is effective for both color images and gray images. The horizon can be extracted not only from fine images captured in fair conditions but also from blurred images captured in cloudy, even foggy days. In order to raise the computational speed to meet real-time requirements, the algorithmic optimization is also discussed in the paper, which is timesaving by narrowing the seeking scope of orientations and adopting the table look-up method. Finally, several experimental results are given to demonstrate the feasibility and robustness of the algorithm.

II. Horizon Extraction Algorithm

First the horizon is considered as a line with the high likelihood of separating the ground from the sky [7]. The assumptions of the horizon extraction algorithm include that the sky is visible and there is a horizon in the images from an on-board forward-looking camera. In this paper, the horizon extraction algorithm is based on the orientation projection method, which includes image preprocessing, orientation selection, projection scope determination, pixel projection calculation, projection direction determination with maximum projection value and horizon estimation.

A. Image Preprocessing

Image preprocessing is the first step for the horizon extraction, which involves noise removing, image enhancement, edge detection and image binaryzation. Image enhancement can enhance the contrast of the image pixels, which is very important for the blurred images captured in unfair days. The histogram balance method is adopted to enhance images.

Containing a lot of useful information, the edge is a very significant representing form of an object, which has a wide applications in image analysis, shape recognition, etc. The horizon can be seen as the edge of the sky in a video image. Thus edge detection is essential to enhance line features of the image and eliminate jagged edges.

Several operators can be used in the edge detection, such as grad operator, Robot operator, Laplace operator, LOG operator, etc. The LOG operator is adopted in this paper, which combines the image sharpness function of the Laplace operator and the smooth filtering function of the Guass operator. The LOG operator combines the image sharpness function of the Laplace operator and the smooth filtering function of the Guass operator. It can both highlight the regions in which the intensity changes rapidly and remove image noises. It can yield good results of edge enhancement. A 5×5 LOG mask is used in this paper. After being processed by the LOG operator, the lines in video images become more clear and distinguishable. The horizon information is protruded.

The orientation projection method is performed on the basis of binary images. So image binaryzation is an essential step in the algorithm. The key factor is the threshold selection. Different methods of selecting threshold will lead to different results. An improper threshold will either introduce much more noise or lose a lot of valuable information of the image, which may bring many troubles to the horizon extraction. In the view of the computational speed of the algorithm, a global threshold

selection method based on the statistical properties of the image is adopted in this paper.

A video image captured from the camera is assumed to be sampled to form a $L \times M$ (352×288, the pixel number of the camera used in our MAV) discrete gray scale image with integer density values from the range $[1, m]$. Suppose the number of the pixels with gray level "i" is n_i. Then the total number of the pixels in the image is given by

$$N = \sum_{i=1}^{m} n_i. \tag{1}$$

The probability of each gray level is

$$P_i = \frac{n_i}{N}. \tag{2}$$

Separate the gray levels into two groups $C_0 = \{1, 2, \ldots, k\}$ and $C_1 = \{k+1, k+2, \ldots, m\}$ by the integer k. Then the probabilities and means of C_0 and C_1 are given by

$$\begin{cases} \omega_0(k) = \sum_{i=1}^{K} P_i \\ \mu_0(k) = \sum_{i=1}^{k} iP_i/\omega_0(k) = \mu(k)/\omega_0(k) \end{cases} \tag{3}$$

$$\begin{cases} \omega_1(k) = \sum_{i=k+1}^{m} P_i = 1 - \omega_0(k) \\ \mu_1(k) = \sum_{i=k+1}^{m} iP_i/\omega_1 = [\mu - \mu(k)]/[1 - \omega_0(k)] \end{cases} \tag{4}$$

where $\mu = \sum_{i=1}^{m} iP_i$ is the statistical mean of the whole image gray levels. According to (3) and (4), we have

$$\mu = \omega_0(k)\mu_0(k) + \omega_1(k)\mu_1(k). \tag{5}$$

The variance between the two groups is

$$\sigma^2(k) = \omega_0(k)[\mu_0(k) - \mu]^2 + \omega_1(k)[\mu_1(k) - \mu]^2. \tag{6}$$

The optimal threshold k is the gray level by which $\sigma^2(k)$ is maximum.

If the term $G(i, j)$ denotes an observed density value of the pixel (i, j), after performing the binary operation for the image by the optimal threshold we have

$$G(i,j) = \begin{cases} 255, & G(i,j) > k \\ 0, & G(i,j) \le k \end{cases}, \quad i = 1, \ldots, L, \quad j = 1, \ldots, M. \tag{7}$$

Black pixels have the density value $G(i, j) = 0$ which constitute the background, while white pixels have the density value $G(i, j) = 255$ which form part of the image.

After image preprocessing, a binary image sequence can be obtained, in which the line information is prominent.

B. Orientation Projection Algorithm

The orientation projection algorithm is performed after image preprocessing. First of all, 32 projection directions from 0°–180° are chosen (0° and 180° are considered as the same direction) in order to balance the computational precision with the speed, which are denoted by the orientation number $m (m = 0, 1, \ldots, 31)$. Then the orientation projection can be made for an image in the selected direction. Now we define the projection value as the number of white pixels along the selected projection direction in the image. The maximum projection value in each projection direction and the position corresponding to the maximum value are recorded. Select the global maximum projection value for all directions. The horizon line can be drawn based on the projection direction and the position where the global maximum projection value is obtained.

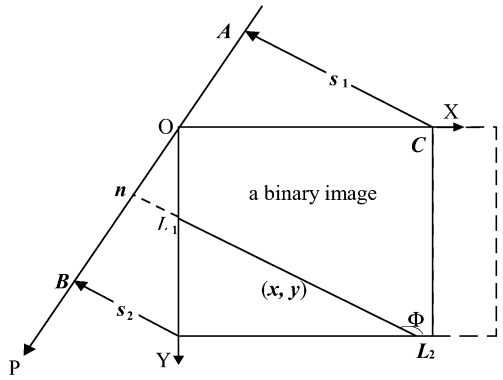

Fig. 1. Sketch map of orientation projection for an image.

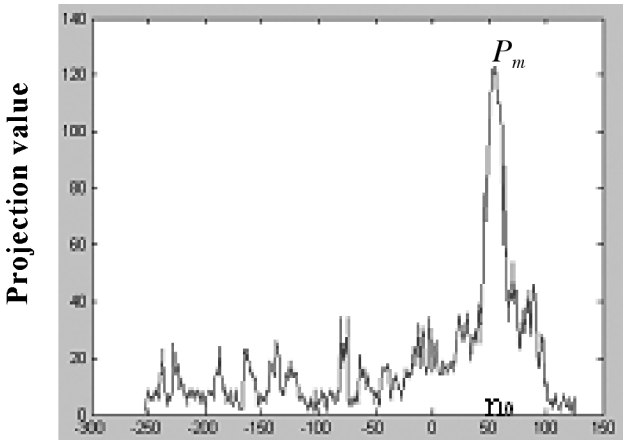

Fig. 2. Pixel projection curve of an image in the projection direction m.

Because the camera was equipped in the left front of the vehicle in our MAV, the propeller influenced the right area of the image. In order to eliminate the disturbance of the propeller and reduce the computational burden, the left square of the image is used to perform projection. The sketch map of orientation projection is illustrated in Fig. 1.

As shown in Fig. 1, two coordinate systems, the image coordinate system and the projection axis coordinate system, are defined. O is the common origin of the two coordinate systems. OX and OY are two axes of the image coordinate system. Φ is the orientation angle dependent on the orientation number m, representing the projection direction. OP is the projection axis, which is perpendicular to the selected projection direction m. L_1L_2 is a line parallel to the selected projection direction, which is vertical to OP. (x, y) is the coordinates of a pixel on L_1L_2. n is the position at which the line L_1L_2 is projected onto OP. A and B are the projection limits.

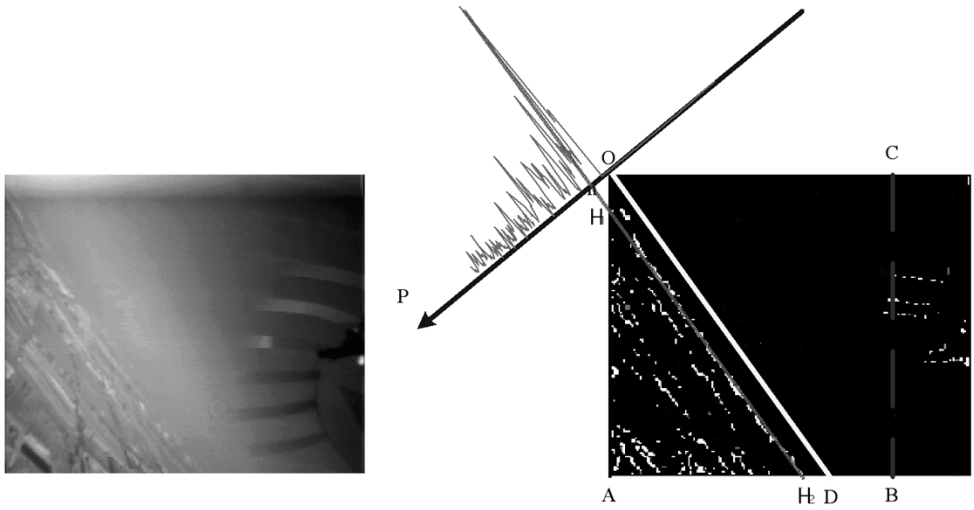

Fig. 3. Original image and the pixel projection result in one direction. (A) An original image captured from the on-board camera. (B) The preprocessed image and the pixel projection result in one direction.

According to the size of the image and the selected projection direction, the projection scope can be limited with the following equations

$$\begin{cases} p(A) = -\sqrt{2}OC \times \cos(\frac{\pi}{4} - \Phi), & 0 \le \Phi \le \frac{\pi}{2} \\ p(B) = 0 \end{cases} \quad (8)$$

$$\begin{cases} p(A) = -OC \times \sin\Phi \\ p(B) = -OC \times \cos\Phi \end{cases}, \quad \frac{\pi}{2} \le \Phi \le \pi \quad (9)$$

where $p(A), p(B)$ are the coordinate values of A and B at the projection axis, respectively.

Project all the pixels of the image to the projection axis along the selected projection direction within the limited scope. The relationship between the projection coordinate n and the coordinates (x, y) of a projected pixel located on L_1L_2 satisfies the following equation.

$$n = -x\sin\Phi - y\cos\Phi, \quad 0 \le \Phi \le \pi. \quad (10)$$

Define $P(x, y)$ is the pixel projection value of the pixel (x, y), we have

$$P(x,y) = \begin{cases} 1, & G(x,y) = 255 \\ 0, & G(x,y) = 0 \end{cases}. \quad (11)$$

If $P_m(n)$ represents the projection value of the image pixels along the line L_1L_2, then

$$P_m(n) = \sum_{(x,y)\in L_1L_2} P(x,y). \quad (12)$$

Fig. 2 shows a pixel projection curve of an image in the selected direction whose orientation number is m. The peak of the projection values P_m occurs at the position n_0. This means that the longest edge in the projection direction passed through n_0. Record the orientation number m, the maximum projection value P_m and the projection position n_0 where the maximum projection value is obtained for further calculations.

Fig. 3 gives an original image and its preprocessed image with the pixel projection curve in one direction. The left image is an original image captured from a forward-looking camera on-board the aircraft. The right one is the preprocessed image with the sketch map of the pixel projection curve in one direction. The line OD represents the projection direction. The curve above the projection axis is the orientation projection curve. The line parallel to OD, which passes through the position where the maximum projection value exists, is possibly the horizon.

Project the image in all directions and we can get a three-dimentional (3-D) graph of the orientation projection as seen in Fig. 4. The three axes denote the projection direction, the projection position and the projection value, respectively. The peak value $P_{\max}$ gives the global maximum projection value of the image in all projection directions. Based on the projection direction m and the position n corresponding with the peak value, the horizon line may be obtained.

In the following, the horizon is written in the mathematical formulation according to the orientation number m and the projection position n of the horizon on the projection axis. See Fig. 1. Suppose L_1L_2 is a horizon line in the image and (x, y) is a point on the horizon. We have

$$\Phi = m \times \frac{\pi}{32} \quad (13)$$

$$y = -xtg\Phi - \frac{n}{\cos\Phi}, \quad \Phi \in \left[0, \frac{\pi}{2}\right) \bigcup \left(\frac{\pi}{2}, \pi\right]. \quad (14)$$

C. Algorithmic Optimization

In order to raise the computational speed to meet real-time requirements, the algorithmic optimization is considered in this paper.

1) Projection Direction Restriction: Since the interval between two successive images in the video sequence is very short, the direction and the position of the horizon in the two images could not change dramatically. Hence, based on the horizon in the previous image, the seeking range of orientations in the latter image can be narrowed.

At the beginning, the orientation projection calculation should be performed in all directions in order to obtain an

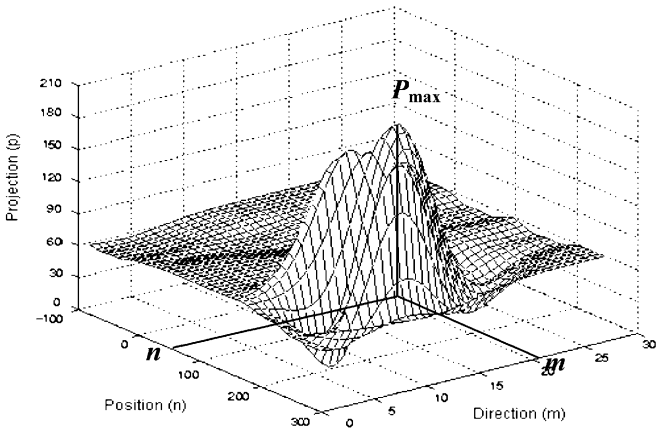

Fig. 4. Three-dimensional graph of orientation projection.

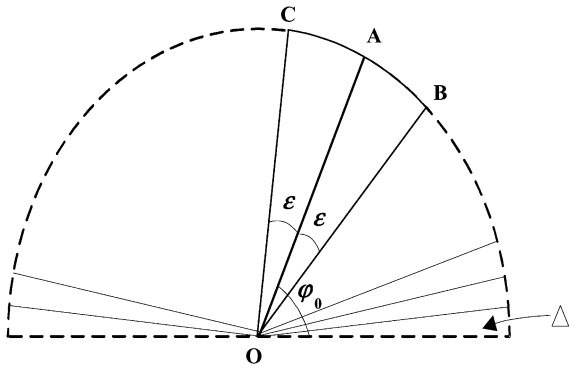

Fig. 5. Illustration of limited seeking scope.

exact result. The seeking step depends on the demands of computational precision and speed.

When the horizon estimation is finished for the first image, the seeking scope of orientations could be reduced based on the direction of the horizon figured out in the former picture.

Fig. 5 is an illustration of limited seeking scope. Suppose OA is the horizon extracted from the former picture, the seeking range of the projection directions described by the orientation angle for the current image could be limited in the sector BOC. In Fig. 5, Δ represents a seeking step. Assume that φ is the projection orientation angle of the current image, we have

$$\varphi_0 - \varepsilon \le \varphi \le \varphi_0 + \varepsilon \tag{15}$$

where φ_0 is the projection orientation angle of the horizon extracted from the former image and ε is a selected seeking scope.

The seeking step could also be augmented reasonably in order to speed up the algorithm.

2) Table Look-Up Algorithm: The table look-up method is also adopted in our algorithm, which is another effective approach to elevate the computational speed. The data that will be used are figured out in advance and saved in a table. These data can be obtained directly from the data table instead of being calculated in the program so as to save time and processing resources.

The improved horizon extraction algorithm can save much more time and the computational speed is raised remarkably.

The horizon determination algorithm presented in this paper can extract horizon lines rapidly and is effective for both color images and gray images. Of course, it should satisfy the assumptions that the sky and ground is distinct, which is a requirement even for people to recognize the horizon, and there exists a horizon in the image. The algorithm will fail in the cases that it is difficult to distinguish the sky and the ground in the blurred images or no horizon is visible in the image when the nose of the MAV is too far up or down in its extreme attitudes. Some control actions should be taken to make the aircraft stable and bring the horizon back into the camera images.

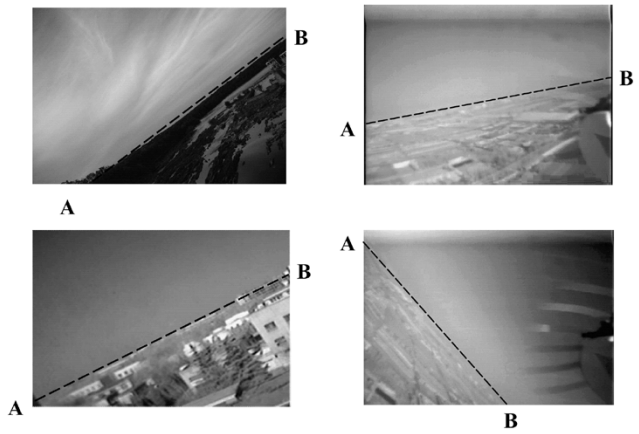

Fig. 6. Horizon extracted from video images.

III. Experimental Results

In our flight test experiments, the video images captured from a forward facing camera on-board the MAV are streamed to a ground computer through a micro video signal transmitting system designed by our research group [10]. All the processing steps are performed in the computer. The micro aircraft is controlled during flight procedure by a human pilot through a standard radio link. The algorithm starts to be operated until the MAV reaches sufficient altitude and the horizon is in the view of the camera. Several hours of video images have been taken from the on-board camera at different times of days under both clear and cloudy conditions, in which the horizon always appears. The target scene in these video images includes buildings, roads, trees, meadows, and pools. For these data, the horizon is correctly identified in nearly 100% of cases. Fig. 6 gives some processing results. The four images are captured in different circumstances. The black dot lines shown in the images are the detected horizon lines. The horizon extraction algorithm is effective for whatever the color images in the left or the gray images in the right. Furthermore, it is available not only in the clear days as shown in the first image but also in the cloudy or even foggy days as shown in the other three ones.

IV. Conclusion

The horizon extraction is, of course, only the first step in a vision-based control system of MAVs, which is currently being developed. The horizon extraction algorithm presented in this paper can determine the horizon rapidly not only from fine images captured in fair conditions but also from blurred images captured in cloudy, even foggy days for both color images and gray images. For the further research, we are endeavouring to

extract more flight parameters based on vision processing of video. Our vision-based research work now focuses on flight parameter extraction, a real-time DSP-based hardware implementation, and a vision-based control and navigation system of MAVs.

REFERENCES

[1] J. M. McMichael and M. S. Francis, Micro Air Vehicles: Toward a New Dimension in Flight.

[2] D. A. Jenkins, P.G. Ifju, M. Abdulrahim, and S. Olipra, "Assessment of controllability of micro air vehicles," in *Proc. 16th Int. Conf. Unmanned Air Vehicle Syst.*, Apr. 2001.

[3] W. R. Davis *et al.*, "Micro air vehicles for optical surveillance," *The Lincoln Lab. J.*, vol. 9, pp. 197–213, 1996.

[4] D. Page, Micro Air Vehicles: Learning from the Birds and Bees.

[5] F. Pipitone, B. Kamgar-Parisi, and R. L. Hartley, "Three dimensional computer vision for micro air vehicles," in *Proc. SPIE 15th Aerosense Symp., Enhanced, and Synthetic Vision*, vol. 4363, 2001, pp. 189–197.

[6] S. Maitra and G. Babb, "Estimation 6 DOF from visual information," in *Proc. SPIE Enhanced and Synthetic Vision*, vol. 3691, 1999, pp. 89–97.

[7] S. M. Ettinger, M. C. Nechyba, P. G. Ifju, and M. Waszak, "Vision-guided flight stability and autonomy for micro air vehicles," in *Proc. IEEE Int. Conf. Intelligent Robots and Systems*, vol. 3, 2002, pp. 2134–2140.

[8] D.-G. Sim *et al.*, "Hybrid estimation of navigation parameters from aerial image sequence," *IEEE Trans. Image Process.*, vol. 8, no. 3, pp. 429–435, Mar. 1999.

[9] S. Furst and E.-D. Dickmanns, "A vision based navigation system for autonomous aircraft," *Robot. Autonomous Syst.*, vol. 28, pp. 173–184, 1999.

[10] M. Jin *et al.*, "Research on the receptive station of a miniature wireless video communication system," in *Proc. 5th Int. Symp. Test Measure.*, 2003, pp. 61–64.

Gui-Qiu Bao was born in Liaoning Province, P.R. China, in 1973. She received the Ph.D. degree in precision instruments and machinery from Tsinghua University, Beijing, P.R. China, in 2004.

Her research interests include image processing and automatic control.

Shen-Shu Xiong (M'02) was born in Liaoning Province, P.R. China, in 1970. She received the B.S.E. degree in computer science and technology and the M.S.E. and Ph.D. degrees in precision instruments and machinery, all from Tsinghua University, Beijing, P.R. China, in 1990 and 1997, respectively.

In 1997, she joined the faculty of the Department of Precision Instruments and Mechanology, Tsinghua University, where she is now an Associate Professor. Her research interests include image processing, automatic control, system identification, and neural networks.

Zhao-Ying Zhou was born in Jiangsu Province, P.R. China, in 1937. He received the B.S.E. degree from the Department of Precision Instruments and Mechanology, Tsinghua University, Beijing, P.R. China, in 1961.

From 1979 to 1981, he was a Visiting Scholar with the Department of Automatic Control, Lund University, Sweden. Currently, he is a Professor with the Department of Precision Instruments and Mechanology, Tsinghua University. His main research interests are in the areas of MEMS and automatic control.

Prof. Zhou is a Member of SPIE.